

**Weak lensing probes of modified gravity**

Fabian Schmidt\*

*Department of Astronomy and Astrophysics, The University of Chicago, Chicago, Illinois 60637-1433, USA  
and Kavli Institute for Cosmological Physics, Chicago, Illinois 60637-1433, USA*

(Received 30 May 2008; published 6 August 2008)

We study the effect of modifications to general relativity on large-scale weak lensing observables. In particular, we consider three modified gravity scenarios:  $f(R)$  gravity, the Dvali-Gabadadze-Porrati model, and tensor-vector-scalar theory. Weak lensing is sensitive to the growth of structure and the relation between matter and gravitational potentials, both of which will in general be affected by modified gravity. Restricting ourselves to linear scales, we compare the predictions for galaxy-shear and shear-shear correlations of each modified gravity cosmology to those of an effective dark energy cosmology with the same expansion history. In this way, the effects of modified gravity on the growth of perturbations are separated from the expansion history. We also propose a test which isolates the matter-potential relation from the growth factor and matter power spectrum. For all three modified gravity models, the predictions for galaxy and shear correlations will be discernible from those of dark energy with very high significance in future weak lensing surveys. Furthermore, each model predicts a measurably distinct scale dependence and redshift evolution of galaxy and shear correlations, which can be traced back to the physical foundations of each model. We show that the signal-to-noise for detecting signatures of modified gravity is much higher for weak lensing observables as compared to the integrated Sachs-Wolfe effect, measured via the galaxy-cosmic microwave background cross-correlation.

DOI: [10.1103/PhysRevD.78.043002](https://doi.org/10.1103/PhysRevD.78.043002)

PACS numbers: 95.30.Sf, 95.36.+x, 98.80.-k, 98.80.Jk

**I. INTRODUCTION**

A number of independent observations, ranging from supernovae to the cosmic microwave background (CMB) and its cross-correlation with foreground galaxies [1–5], have now firmly established that the expansion of the Universe is accelerating, and that a purely matter-dominated universe is not consistent with measurements. Commonly, these observations are ascribed to an additional smooth stress-energy component, “dark energy” (DE), pervading the Universe [6]. However, instead of attributing the accelerated expansion to our lack of understanding of the constituents of the Universe, one can take the alternative approach and attribute it to our lack of understanding of gravity on cosmological scales. For example, an effective weakening of gravity on the largest scales could explain the accelerated expansion and other cosmological observations without invoking an additional smooth “dark” component. Several such modified gravity scenarios have been proposed. The difficulty in constructing a consistent theory of gravity which preserves the success of general relativity (GR) in the Solar System and the early Universe has however limited the number of proposed theories to only a handful.

Seen from a fundamental physics point of view, the two approaches of general relativity coupled with a smooth dark energy (GR + DE) and modified gravity are apparently quite distinct. However, there is enough freedom in both scenarios to match any given expansion history of the

Universe. Thus, the expansion history, measured primarily with supernovae and the CMB, is not sufficient to distinguish between these two “fundamentally different” scenarios.

Going beyond the smooth background Universe offers a multitude of additional observables probing the evolution of structure formation in the Universe. For the purpose of constraining modified gravity, the evolution of the cosmological gravitational potentials, and their relation to the matter overdensities and velocities are the most sensitive probes [7–10]. Several such observational tests of gravity have been proposed: the integrated Sachs-Wolfe (ISW) effect [11–15] directly probes the evolution of the potentials on horizon-size scales. While quite sensitive as a probe of gravity, it is restricted to large scales, and offers only a limited amount of signal-to-noise. The *matter power spectrum* probes the growth of matter perturbations on a range of scales. While it can be measured to high precision and to very small scales, and hence offers a large amount of information, it is affected by the nonlinearities of structure formation, and galaxy bias, which are not well understood for modified gravity models. A cleaner method of probing gravity with galaxies is using *velocity correlations* [7,16,17]. In principle, these tests can isolate signatures of modified gravity. However, they will be challenging to perform observationally.

Several deep, wide-field galaxy surveys are in the planning stage which are designed to measure galaxy counts and weak lensing shear with unprecedented accuracy. Galaxy and shear correlations can be used to measure the expansion history and growth of structure in the Universe

\*fabians@oddjob.uchicago.edu

to high precision. Additionally, the potential of weak lensing observables to probe gravity has been shown in [7,18–21]. In this paper, we investigate the constraints on modified gravity theories to be expected from galaxy and shear correlations in future surveys. Since weak lensing is caused by the potential wells along the line of sight, it can be used to measure the scale dependence and cosmological evolution of these potentials. In addition, correlating foreground galaxies with the shear of background galaxies offers a test of the matter-potential relation. We will show that future weak lensing surveys will place very tight constraints on gravity. In other words, they will perform stringent tests of the smooth dark energy scenario, which will have to match all of the weak lensing observables in order to remain a viable model.

Regarding the potential of these precision tests, it is important to keep several caveats in mind: first, the non-linear evolution in modified gravity models is not yet understood in a realistic cosmological context. Hence, in this paper we will limit ourselves to scales where linear theory is appropriate. Second, correlations involving galaxy number counts are affected by the galaxy bias, which is *a priori* unknown. We will point out how the effects of bias can hopefully be disentangled from modified gravity effects. Third, it is always possible to find a general, non-smooth dark energy model which mimics the predictions of any given modified gravity model [22,23]; note that such a DE model will have significant density and anisotropic stress perturbations on subhorizon scales.

In this paper, we will study three different modified gravity scenarios, focusing on their predictions for lensing observables: (i)  $f(R)$  gravity [24–28]; (ii) the Dvali-Gabadadze-Porrati (DGP) model [29–31]; and (iii) -tensor-vector-scalar theory (TeVeS) [32]. While the first two models are able to achieve accelerated expansion without dark energy, TeVeS is designed to explain observations without dark matter by showing MOND-behavior in certain regimes. These three theories encompass very different approaches to the problem of constructing a consistent theory of gravity. Hence, it is interesting to determine not only whether observations can detect departures from GR, but also whether they would be able to discriminate among different modified gravity scenarios.

In addition to predicting a late-time accelerated expansion of the Universe, all these models have been designed to approach GR in the high-curvature regime, which applies to the Solar System as well as the early Universe. In this way, the models pass Solar System tests while making predictions close to the standard cosmological model for the CMB and big bang nucleosynthesis.

Weak lensing probes the growth of large-scale structure which is sensitive to the background expansion history, as the expansion rate enters the evolution equations of perturbations. Since two of the models discussed here (DGP and TeVeS) predict expansion histories somewhat different

from  $\Lambda$ CDM, we compare them with smooth dark energy models designed to mimic the expansion history of these models by employing a suitable equation of state  $w(a)$ . Deviations in the weak lensing predictions of DGP and TeVeS from the corresponding dark energy model are then solely due to modified gravity effects on the growth of structure and the matter-potential relation, and independent of the exact expansion history.

The structure of the paper is as follows. In Sec. II, general expressions for galaxy and shear correlations applicable to modified gravity are given, and we point out the different channels through which modified gravity can affect the observables. We also present a cosmological test of the Poisson equation using weak lensing and galaxy correlations. In Sec. III, we briefly describe the modified gravity models studied here, and outline the characteristics which determine their lensing predictions. We then present forecasts for galaxy-shear and shear-shear correlations in future surveys in Sec. IV, showing the deviations of the modified gravity predictions from those of GR + DE, as well as the expected signal-to-noise in actual surveys. We conclude in Sec. V.

## II. WEAK LENSING CORRELATIONS

### A. Weak lensing in modified gravity

In this section, we summarize the lensing observables considered in this paper, generalizing the standard expressions to the case of modified gravity. We assume a flat Universe throughout. Our metric convention is [33]:

$$ds^2 = a^2(\eta)[-(1 + 2\Psi)d\eta^2 + (1 + 2\Phi)dx^2], \quad (1)$$

where  $a(\eta)$  is the scale factor,  $\eta$  denotes conformal time, and  $\Phi$ ,  $\Psi$  are the cosmological potentials. In general relativity (GR),  $\Phi = -\Psi$  in the absence of anisotropic stress, which is the case at late times in  $\Lambda$ CDM and most dark energy models. In addition, the potentials are conventionally reexpressed in terms of the matter overdensity using the Poisson equation. In case of modified gravity, both of these assumptions do not necessarily hold. In the following we give generalized expressions for the different observables which apply to the case of modified gravity (see also [7,18]). We restrict ourselves to linear perturbations valid on large scales ( $k \lesssim 0.1$  h/Mpc). Since the  $f(R)$  and DGP models recover the GR + DE limit at early times in the matter-dominated epochs, it is convenient to refer observables to the matter overdensity at high redshift  $z_m$ . For definiteness, we take  $z_m = 50$ . Then, for any viable  $f(R)$  and DGP model,  $P(k, z_m)$  is identical to that expected in GR.

Weak lensing surveys use the observed ellipticities of galaxies to reconstruct a map of the cosmic shear, which can then be used to infer the convergence  $\kappa$  [34,35]. In the following, we will use the terms convergence and shear interchangeably, understanding that they are reconstructed from observed galaxy ellipticities. Using standard approx-

imations, the convergence in the direction  $\hat{\mathbf{n}}$ , given by the Laplacian of the projected lensing potential, is expressed as a line of sight integral to the source at redshift  $z_s$ :

$$\kappa(\hat{\mathbf{n}}) = - \int_0^{z_s} \frac{dz}{H(z)} \nabla^2 \Phi_-(\mathbf{x}(z), z) W_L(\chi_s, \chi(z)), \quad (2)$$

where  $\chi(z)$  is the comoving distance out to redshift  $z$ ,  $H(z) = \frac{da}{dt}/a$  is the expansion rate,  $\Phi_- \equiv 1/2(\Phi - \Psi)$ ,  $\nabla^2$  denotes the Laplacian in terms of comoving coordinates, and the lensing weight function is given by:

$$W_L(\chi_s, \chi) = \frac{\chi}{\chi_s} (\chi_s - \chi). \quad (3)$$

Hence, the convergence is sensitive to the potential  $\Phi_-$  in a range of distances centered around  $\chi \sim \chi_s/2$ . Note that in the case of GR and smooth dark energy (referred to as ‘‘GR + DE’’ in the following),  $\Phi_- = \Phi = -\Psi$ , and we can apply the Poisson equation:

$$\nabla^2 \Phi_-^{\text{GR+DE}} = 4\pi G a^2 \rho_m \delta = \frac{3}{2} \Omega_m H_0^2 a^{-1} \delta \quad (4)$$

In modified gravity, this equation does not hold anymore, and we define a generalized ‘‘Poisson factor’’  $D_{\Phi_-}$  relating the potential  $\Phi_-$  to the matter overdensity  $\delta$  in Fourier space:

$$D_{\Phi_-} \equiv \frac{\Phi_-(k, z)}{\delta(k, z)} \stackrel{\text{GR+DE}}{=} \frac{3}{2} \Omega_m \frac{H_0^2}{k^2} a^{-1} \quad (5)$$

Apparently, a departure of the Poisson factor  $D_{\Phi_-}$  from its expected value in general relativity is a signature of the modification of the Poisson equation in alternative gravity theories (for a discussion of general, nonsmooth dark energy models, see Sec. III D). In addition, the growth of potential and matter perturbations is affected by modified gravity. The growth factor of matter, which we normalize at  $z = z_m = 50$  so that  $D_m(k, z) \equiv \delta(k, z)/\delta(k, z = z_m)$ , becomes scale-dependent in many modified gravity models. We can combine the growth of structure and the Poisson equation to obtain:

$$\frac{\Phi_-(k, z)}{\delta(k, z = z_m)} = D_{\Phi_-}(k, z) D_m(k, z). \quad (6)$$

This allows us to express the galaxy-galaxy, galaxy-shear, and shear-shear correlation coefficients,  $C^{g_g}(\ell)$ ,  $C^{g\kappa}(\ell)$ ,  $C^{\kappa\kappa}(\ell)$  as follows:

$$\begin{aligned} C^{g_g}(\ell) &= \frac{2}{\pi} \int dk k^2 P(k, z_m) \\ &\times \int dz b_i W_{g_i}(z) D_m(k, z) j_\ell(k\chi(z)) \\ &\times \int dz' b_j W_{g_j}(z') D_m(k, z') j_\ell(k\chi(z')), \quad (7) \end{aligned}$$

$$\begin{aligned} C^{g_i\kappa_j}(\ell) &= \frac{2}{\pi} \int dk k^2 P(k, z_m) \\ &\times \int dz b_i W_{g_i}(z) D_m(k, z) j_\ell(k\chi(z)) \\ &\times \int dz' W_{\kappa_j}(z') k^2 D_{\Phi_-}(k, z') \\ &\times D_m(k, z') j_\ell(k\chi(z')), \quad (8) \end{aligned}$$

$$\begin{aligned} C^{\kappa_i\kappa_j}(\ell) &= \frac{2}{\pi} \int dk k^2 P(k, z_m) \\ &\times \int dz W_{\kappa_i}(z) k^2 D_{\Phi_-}(k, z) D_m(k, z) j_\ell(k\chi(z)) \\ &\times \int dz' W_{\kappa_j}(z') k^2 D_{\Phi_-}(k, z') D_m(k, z') j_\ell(k\chi(z')). \quad (9) \end{aligned}$$

Here,  $P(k, z_m)$  is the matter power spectrum at early times  $z = z_m$ , which in the case of the  $f(R)$  and DGP models is the same as for a GR + smooth DE model with the same expansion history. The indices  $i, j$  denote different redshift bins, i.e.,  $W_{g_i}(z)$  is the galaxy redshift distribution for bin  $i$ , normalized to 1,  $b_i$  is the galaxy bias for the same bin, and the shear weighting function of redshift bin  $j$ ,  $W_{\kappa_j}$ , is given by:

$$W_{\kappa_j}(z) = \frac{1}{H(z)} \int_z^\infty dz_s W_L(\chi(z_s), \chi(z)) W_{g_j}(z_s). \quad (10)$$

For  $\ell \geq 10$ , we can apply the Limber approximation [36], which simplifies the expressions considerably:

$$\begin{aligned} C^{g_i g_j}(\ell) &= \int dz \frac{H(z)}{\chi^2(z)} b_i W_{g_i}(z) b_j W_{g_j}(z) \\ &\times [D_m^2(k, z) P(k, z_m)]_{k=(\ell+1/2)/\chi(z)}, \quad (11) \end{aligned}$$

$$\begin{aligned} C^{g_i \kappa_j}(\ell) &= \int dz \frac{H(z)}{\chi^2(z)} b W_{g_i}(z) W_{\kappa_j}(z) \\ &\times [D_{\Phi_-}(k, z) D_m^2(k, z) k^2 P(k, z_m)]_{k=(\ell+1/2)/\chi(z)}, \quad (12) \end{aligned}$$

$$\begin{aligned} C^{\kappa_i \kappa_j}(\ell) &= \int dz \frac{H(z)}{\chi^2(z)} W_{\kappa_i}(z) W_{\kappa_j}(z) \\ &\times [D_{\Phi_-}^2(k, z) D_m^2(k, z) k^4 P(k, z_m)]_{k=(\ell+1/2)/\chi(z)}. \quad (13) \end{aligned}$$

Weak lensing correlations thus depend on cosmology through three distinct channels: (i) the background expansion history, via  $H(z)$  and  $W_L(\chi_s, \chi(z))$ ; (ii) the growth of perturbations and the Poisson equation, through  $D_m(k, z)$  and  $D_{\Phi_-}(k, z)$ ; and (iii) the matter power spectrum at early times,  $P(k, z_m)$ . In case general relativity holds and the accelerated expansion is due a smooth dark energy, only the expansion history (i) is affected by the dark energy, i.e.

modified from  $\Lambda$ CDM. In the case of the late-time acceleration modified gravity models  $f(R)$  and DGP, both channels (i) and (ii) are affected. And the TeVeS model without dark matter modifies (i), (ii), as well as (iii) from the  $\Lambda$ CDM case.

In this paper, we want to illuminate how weak lensing correlations are sensitive to these three channels, both in redshift evolution and in scale dependence. Clearly, it is crucial to separate these effects in order to distinguish between GR + DE and modified gravity; in addition, testing  $D_m(k, z)$ ,  $D_{\Phi_-}(k, z)$ , and  $P(k, z_m)$  separately will allow to distinguish between different modified gravity scenarios.

The galaxy-shear correlation is proportional to the *a priori* unknown bias of the foreground galaxies. Assuming that the bias is scale-independent on linear scales, one can marginalize over this parameter for a given galaxy sample. An alternative is to consider the reduced galaxy-shear correlation  $R^{g\kappa}(\ell)$ , defined by:

$$R^{g_i\kappa_j}(\ell) \equiv \frac{C^{g_i\kappa_j}(\ell)}{\sqrt{C^{g_i g_i}(\ell)}}. \quad (14)$$

For redshift bins that are not too wide, the linear galaxy bias drops out of this expression, so that  $R^{g\kappa}$  is independent of  $b_i$ . Since it is not straightforward to compute the errors on this quantity, we will for simplicity only consider the galaxy-shear correlation divided by the bias,  $C^{g\kappa}(\ell)/b$ , in this paper. In any case, we do not expect the constraints to be degraded very significantly when considering  $R^{g\kappa}$  instead of  $C^{g\kappa}$ .

On small scales  $k \sim 0.1$  h/Mpc and above, the density contrast grows to order unity, and nonlinearities in the formation of structure become important. Furthermore, all of the modified gravity theories studied here employ nonlinear equations of motion which are expected to restore gravity to general relativity in high-density environments [32,37–39]. These mechanisms have been studied in special cases, e.g. spherically symmetric and/or static cases [32,37]; however, the details of cosmological structure formation in the nonlinear regime have not been studied in the case of modified gravity. Hence, we will restrict our discussion to linear scales in this paper.

### B. A cosmological probe of the Poisson equation

Recently, techniques have been proposed to isolate the geometrical factors in weak lensing correlations from the growth of structure, bias, and matter power spectrum (shear ratios, or "cosmography" [40,41]). Because of the separation of geometry from growth effects, cosmographic techniques apply equally well in modified gravity theories, i.e. when using the generalized expressions (11)–(13).

A similar approach as for cosmography can be used to separate out the effect of a modified Poisson equation from the growth factor and matter power spectrum. Observing a modification of the Poisson equation on cosmological

scales would constitute a "smoking gun" for deviations from the GR + smooth dark energy scenario. Consider a very narrow galaxy redshift distribution centered around  $z_f$ . Then, the galaxy-galaxy and galaxy-shear correlation coefficients become:

$$C^{gg}(\ell) \simeq \frac{H(z_f)}{\chi_f^2} b^2 [D_m^2(k, z) P(k)]_{k=(\ell+1/2)/\chi_f}, \quad (15)$$

$$\chi_f \equiv \chi(z_f),$$

$$C^{g\kappa}(\ell) \simeq \frac{H(z_f)}{\chi_f^2} b W_\kappa(z_f) \times [D_{\Phi_-}(k, z) D_m^2(k, z) k^2 P(k)]_{k=(\ell+1/2)/\chi_f}. \quad (16)$$

With this simplifying assumption, ratios of weak lensing correlations can be used to isolate the effect of a modified Poisson equation:

$$\begin{aligned} \mathcal{P}(\ell) &\equiv \frac{C^{g\kappa}(\ell)}{C^{gg}(\ell)} \\ &\simeq b^{-1} H_0^2 W_\kappa(z_f) \left( \frac{k^2}{H_0^2} D_{\Phi_-}(k, z_f) \right)_{k=(\ell+1/2)/\chi_f} \\ &\quad \times \stackrel{\text{GR+DE}}{=} \frac{3}{2} \Omega_m b^{-1} H_0^2 W_\kappa(z_f) (1 + z_f). \end{aligned} \quad (17)$$

These ratios divide out the dependency on the matter power spectrum and growth factor; they still depend on the expansion history, although not very strongly, via  $\chi_f$  and the lensing weight function  $W_\kappa(z_f)$ . On linear scales,  $\mathcal{P}(\ell)$  is independent of scale in GR + DE, due to the scale-independence of both  $k^2 D_{\Phi_-}$  and bias  $b$ . In contrast, a scale-dependence is expected for gravity theories which modify the Poisson equation. Hence, measuring  $\mathcal{P}(\ell)$  as a function of scale  $\ell$  would constitute a robust test of the Poisson equation on large scales. See section III D for a discussion of the effect of nonsmooth dark energy.

### III. MODIFIED GRAVITY MODELS

In this section, we briefly present the modified gravity models and parameters adopted in this paper, and discuss the qualitative expectations for their lensing predictions. First, let us discuss general constraints applicable to any theory of gravity. In any metric theory of gravity that conserves energy-momentum, the evolution of superhorizon perturbations is essentially defined by the expansion history alone [10]. This can be understood in the "separate universes" picture: a superhorizon curvature perturbation behaves essentially as a separate Friedmann-Robertson-Walker universe with a constant small curvature. Hence, the evolution of superhorizon curvature perturbations in modified gravity models is the same as in GR (given the same expansion history) [22,23]. Once a scale-independent superhorizon relation between the metric potentials  $\Phi$  and

$\Psi$  has been supplied by a theory, the evolution of  $\Phi$ ,  $\Psi$  is fixed on superhorizon scales. In the opposite limit, when a mode is well within the horizon, one can apply the quasi-static approximation, neglecting time derivatives with respect to spatial gradients. In this regime, the potentials  $\Phi$ ,  $\Psi$  are given by a modified Poisson equation which again is determined by the theory.

Recently, Hu and Sawicki [22] presented a parametrization of modified gravity theories which is based on the superhorizon and quasistatic regimes, with a suitable interpolation between both. They showed that this ‘‘Parametrized Post-Friedmann’’ (PPF) approach reproduces the predictions of the late-time acceleration  $f(R)$  and DGP models well, with only few model-dependent functions. Several alternative parametrizations of modified gravity have been proposed [7–9,17,23]. The PPF parametrization is most useful for us in that it describes the  $f(R)$  and DGP models with suitable parameters.

The two main model-dependent quantities with impact on cosmological observables are (in the notation of [22]), (i) the metric ratio  $g(k, z)$ , given by:

$$g(k, z) \equiv \left. \frac{\Phi + \Psi}{\Phi - \Psi} \right|_{k,z}, \quad (18)$$

and (ii) the rescaling  $f_G(z)$  of the Newton constant in the Poisson equation [Eq. (4)] on subhorizon scales:

$$G_{\text{eff}}(z) = \frac{G}{1 + f_G(z)}. \quad (19)$$

Note that for GR coupled with a smooth dark energy,  $g = f_G = 0$  at late times. Thus,  $f_G$  influences  $D_{\Phi_-}$  directly, by rescaling the GR value by  $1/(1 + f_G)$ . The metric ratio  $g$  influences the evolution of cosmological perturbations [22,23]: if  $g > 0$ , i.e.  $\Phi + \Psi > 0$ , the potentials decay faster during the epoch of onsetting acceleration than in the GR limit. Conversely, for  $g < 0$  the potential decay is slowed down and, for sufficiently negative  $g$ , inverted into a potential growth. From Eqs. (11)–(13), we expect this suppressed or enhanced growth of perturbations to lead to potentially observable effects in the weak lensing correlations.

### A. $f(R)$ model

In  $f(R)$  gravity, the Einstein-Hilbert action is modified by adding a certain function of the Ricci scalar,  $f(R)$ , to the gravitational part of the Lagrangian [24–28,42–45]:

$$S_{\text{EH}} = \frac{1}{16\pi G} \int d^4x \sqrt{-g} [R + f(R)]. \quad (20)$$

In the case of  $f(R) = C = \text{const}$ , we recover  $\Lambda$ CDM, i.e. GR with a cosmological constant  $\Lambda = -C/2$ . A linear function  $f(R)$ , so that  $f_R \equiv df/dR$  is a constant, simply amounts to a rescaling of Newton’s constant,  $G \rightarrow G/(1 + f_R)$ . Thus, a nontrivial modification of gravity is linked to a nonzero second derivative of  $f$ . The dimensionless field

$f_R \equiv df/dR$  then appears as an additional scalar degree of freedom in the modified Einstein equations.

Different functional forms of  $f(R)$  have been proposed in the literature. They generally satisfy the asymptotic relation  $f(R) \rightarrow 0$  for  $R \rightarrow \infty$ , so that GR is in principle restored in the high-curvature limit, which applies to the Solar System as well as the early Universe. Note that Solar System constraints strongly limit the possible choices of  $f$  [38,42,45]. In addition,  $d^2f/dR^2$  should be positive in order to achieve a stable high-curvature limit [26,43]. For this paper, we adopt the implicit definition of  $f(R)$  proposed in [26]. Since the background curvature  $R$  is fixed as a function of  $a$  for a given expansion history  $a(t)$ , the function  $f(R(a))$  can be determined from the modified Friedmann equations, which are obtained by applying the modified Einstein equations to the FRW metric. We assume the expansion history of our fiducial  $\Lambda$ CDM model, defined by  $\Omega_m = 0.27$ ,  $\Omega_\Lambda = 0.73$ ,  $\Omega_b = 0.046$ ,  $h = 0.7$ ,  $n_s = 0.95$ . For the power spectrum normalization, we use the CMB normalization of the primordial curvature perturbations given by  $\delta_\zeta = 4.58 \times 10^{-5}$  at  $k = 0.05 \text{ Mpc}^{-1}$ , as in the case of the  $\Lambda$ CDM model. This is motivated by the fact that this  $f(R)$  model makes definite predictions for the CMB (i.e., identical to  $\Lambda$ CDM), whereas measurements of the power spectrum amplitude today, e.g. using the power spectrum of galaxies, are affected by gravitational nonlinearities, a regime where definite predictions for modified gravity are still outstanding.

The amplitude of the field  $f_R$ , and correspondingly of the modification to gravity, is most conveniently parametrized in terms of the parameter  $B_0 = B(a = 1)$ , where  $B(a)$  is a function proportional to the second derivative of  $f$ :

$$B(a) \equiv \frac{d^2f/dR^2}{1 + f_R} R' \frac{H}{H'}, \quad (21)$$

where  $R(a)$  is the Ricci scalar of the FRW background, which in turn can be expressed in terms of the Hubble rate  $H(a)$  and its derivatives, and primes denote derivatives with respect to  $\ln a$ . Thus, the evolution of  $f(R)$  in the background is fixed by the expansion history together with  $B_0$ , and we then proceed to calculate the evolution of matter perturbations and potentials using the PPF parametrization presented in [22].

For a positive value of  $B$ , necessary for stability in the high-curvature limit,  $f(R)$  models generically predict a negative  $\Phi + \Psi$ , i.e., a metric ratio  $g < 0$ . On superhorizon scales,  $g$  is of order  $-B$ , and grows to a value of  $-1/3$  on small scales. The negative potential ratio leads to a slower decay of the potentials during the acceleration epoch, and hence a smaller growth suppression of matter perturbations (Fig. 1, left panel) with respect to  $\Lambda$ CDM. Having fixed the fluctuation amplitude at early times through the CMB, we thus expect an increased weak lensing signal from the  $f(R)$  model.

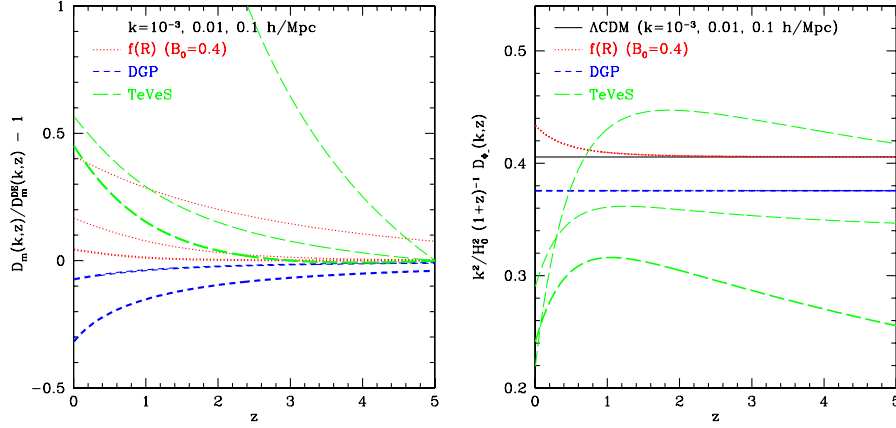


FIG. 1 (color online). Left panel: Deviation of the growth factor  $D_m(k, z)$  from a GR + DE model with the same expansion history, for three different modified gravity models:  $f(R)$  (red/dotted line; using a value of  $B_0 = 0.4$ ), DGP (blue/short-dashed line), TeVeS (green/long-dashed line; normalized to 1 at  $z = 5$  for clarity). The three lines show different scales:  $k = 10^{-3}$  h/Mpc (thick line),  $k = 0.01$  h/Mpc (medium line), and  $k = 0.1$  h/Mpc (thin line). Right panel: The Poisson factor  $D_{\Phi_-}$  [Eq. (5)] scaled by  $k^2/H_0^2/(1+z)$ , which reduces to  $3\Omega_m/2$  in the case of an unmodified Poisson equation, as a function of redshift for  $\Lambda$ CDM and modified gravity models. The lines correspond to the same scales as in the left panel.

As pointed out above, the gravitational constant is rescaled by  $1/(1+f_R)$  in  $f(R)$  models. Since  $f(R) < 0$  to achieve acceleration,  $G_{\text{eff}} > G$  in  $f(R)$  gravity, and hence  $D_{\Phi_-}$  is larger than its  $\Lambda$ CDM value (right panel of Fig. 1). However, this effect is quite small, at the percent level, for observationally allowed models. For the weak lensing forecasts below, we adopt a value of  $B_0 = 0.1$ , leading to a field amplitude today of  $f_R(a=1) = -0.017$ . For purposes of presentation, we use the larger value of  $B_0 = 0.4$  for the plots in Fig. 1.

### B. DGP model

In the Dvali-Gabadadze-Porrati model [29–31], all matter and nongravitational interactions are confined to a  $(3+1)$ -dimensional “brane” embedded in  $(4+1)$ -dimensional space. Only gravity is five-dimensional, and the effects of the large extra dimension become noticeable at the crossover scale  $r_c = G^{(5)}/2G^{(4)}$ , where  $G^{(5)}$  is the gravitational constant in five dimensions, and  $G^{(4)}$  is the usual four-dimensional gravitational constant. The crossover scale  $r_c$  is the only free parameter of the model. One of the two possible branches of the model naturally leads to an accelerated expansion when the horizon scale  $c/H(z)$  reaches  $r_c$ . The expansion history in the DGP model is somewhat different than  $\Lambda$ CDM. It is given by [30]:

$$H(z) = H_0(\sqrt{\Omega_{rc}} + \sqrt{\Omega_{rc} + \Omega_m a^{-3}}), \quad (22)$$

where  $\Omega_{rc} = 1/(4r_c^2 H_0^2)$ , and, for a flat universe,  $\Omega_{rc} = (1 - \Omega_m)^2/4$ . Here, we adopt  $\Omega_m = 0.25$  and  $h = 0.66$ , as determined from fitting Supernova distances and the CMB [14], corresponding to  $r_c H_0 \approx 1.78$ . For the same reasons as in the case of the  $f(R)$  model, we assume a primordial power spectrum normalization of  $\delta_\zeta = 4.58 \times 10^{-5}$  at

$k = 0.05 \text{ Mpc}^{-1}$  for the DGP model. For the evolution of perturbations in DGP, effects from the 5D nature of gravity, namely, perturbations in the extrinsic curvature of the brane, have to be taken into account in order to close the perturbation equations [46,47]. Here, we again employ the interpolation based on the PPF parametrization given in [22]. In order to compare the DGP predictions with those from GR + DE, we use a dark energy model with an equation of state  $w_{\text{eff}}(a)$  which exactly mimics the expansion history of the DGP model.

The DGP model has a positive metric ratio  $g$  which grows proportional to  $1/(Hr_c)$  and is of order unity at  $z = 0$ ; it is only weakly scale-dependent for subhorizon scales. The positive  $g$  leads to an enhanced potential decay with respect to GR + DE [14], as is apparent in Fig. 1 (left panel). Correspondingly, we expect a reduced lensing signal for the DGP model. Note that the decay of the potentials sets in at considerably higher redshifts,  $z \sim 5$ , than in GR + DE. This is because  $w_{\text{eff}} \approx -1/2$  in the DGP model for  $z \gtrsim 1$  [48]. The Poisson equation is not modified in the DGP model. However, as the Poisson ratio  $\mathcal{P}(\ell)$  is proportional to  $\Omega_m$  [Eq. (17)], the prediction for the DGP model shows a scale-independent departure due to the slightly smaller value of  $\Omega_m$  adopted for this model (right panel of Fig. 1). In contrast to the simple DGP model considered here, generalized braneworld-inspired modified gravity models can show a modified Poisson equation [49].

### C. TeVeS

The TeVeS model [32] is a relativistic metric theory of gravity which, as the models presented above, reduces to general relativity in the high-density, high acceleration regime. However, in the high-density, weak acceleration regime, it behaves like modified Newtonian dynamics

(MOND, [50]). The MOND force law can explain galactic rotation curves without invoking dark matter. TeVeS generalizes this idea by adding an additional vector field ( $V$ ) and scalar field ( $S$ ) in such a way that the same effect of dark matter apparently seen in dynamics is also seen in gravitational lensing. Hence, TeVeS can be taken as an attempt to explain all cosmological observables without any dark matter of unknown nature.

For this paper, we adopt the “neutrino model” from [15]. The matter content in this model is given by baryons,  $\Omega_b = 0.05$ , and neutrinos,  $\Omega_\nu = 0.17$ , with a cosmological constant given by  $\Omega_\Lambda = 0.78$ , in order to match the observed expansion history. This model has been shown to be in acceptable agreement with CMB and matter power spectrum observations [51]. While the current TeVeS model uses a cosmological constant to achieve acceleration, related theories invoking vector fields have been proposed which lead to acceleration without a cosmological constant [52]. The evolution equations of linear cosmological perturbations in TeVeS have been derived in [51,53–55]. In order to satisfy big bang nucleosynthesis bounds, the TeVeS scalar field is constrained to small values throughout cosmological history, and neither significantly contributes to the background expansion nor the growth of perturbations. In contrast, perturbations of the timelike vector field exhibit a growing mode which in turn boosts the growth of matter perturbations [54]. Hence, the perturbations of the vector field in TeVeS play the role of seeds of structure formation in the absence of dark matter. The vector degree of freedom is formed by the spatial components of the timelike vector field, which couple to the spatial part of the metric. Hence, the growing vector field only affects the potential  $\Phi$ , which leads to a nonzero  $\Phi + \Psi < 0$ , i.e.  $g < 0$  [54]. As in the case of the  $f(R)$  model, this produces a slower decay, or even growth, of the potentials at late times. However, the power spectrum at earlier times is lower than that of  $\Lambda$ CDM due to the considerably different history of structure formation in TeVeS.

In addition to their effect on the potential ratio, the vector perturbations also appear on the right-hand side of the Poisson equation [15], and even dominate the matter perturbations on small scales. This effect can be seen in the “Poisson factor” (Fig. 1, right panel): on large scales (thick line), the value is significantly smaller than in  $\Lambda$ CDM due to the smaller  $\Omega_m$  in TeVeS without dark matter. Going to smaller scales,  $D_{\Phi_-}$  grows and eventually overtakes the  $\Lambda$ CDM value due to the increasing contribution of vector perturbations [15]. Thus, the Poisson factor in TeVeS shows a characteristic scale dependence and redshift evolution, which should be observable in the correlation ratio  $\mathcal{P}(\ell)$  defined in Sec. II B. We return to this in Sec. IV D.

The TeVeS modifications to GR are somewhat more severe than those from the late-time accelerating models

$f(R)$  and DGP; a simple parametrization in terms of  $g(k, z)$  and  $f_G(z)$  does not exist (yet) for this model. Since the TeVeS model used here has a slightly different expansion history than  $\Lambda$ CDM, we compare it with an effective GR + DE model with the same expansion history.

#### D. Comparison with general dark energy models

In the previous sections we pointed out the two main physical quantities affected by gravity, aside from the expansion history: the growth factor of matter perturbations,  $D_m(k, z)$ , and the matter-potential relation,  $D_{\Phi_-}(k, z)$ . In modified gravity, they are influenced by a nonzero metric ratio  $g$ , and a rescaling of the gravitational constant or additional degrees of freedom appearing in the Poisson equation. Can these signatures possibly be mimicked by a general dark energy model?

Within GR, anisotropic stress perturbations are the only source of differing cosmological potentials. In order to achieve a given metric ratio  $g(k, z)$ , so that  $\Phi + \Psi = g\Phi_-$ , one would need components of the dimensionless anisotropic stress perturbation  $\Pi$ , at late times, of the order of [23]:

$$\Pi(k, z) \sim \frac{ak^2}{H_0^2} g(k, z)\Phi_-(k, z). \quad (23)$$

Clearly, the components of the dark energy anisotropic stress tensor have to be large on small scales in order to produce the order unity values of  $g$  predicted by modified gravity theories. Any neutrino contribution to  $\Pi$  will be very small at late times. In addition, dark energy density perturbations would also add a contribution of the order of  $\rho_{\text{DE}}\delta_{\text{DE}}/(\rho_m\delta)$  to the Poisson ratio  $\mathcal{P}(\ell)$  introduced in Sec. II B. While the dark energy properties necessary to emulate modified gravity seem not to be very natural ones, it is not possible to place stringent constraints on general dark energy models, in lack of an underlying theory. In the linear regime, the two functions  $\delta_{\text{DE}}(k, z)$  and  $\Pi(k, z)$  are sufficient to emulate any given modified gravity model. However, one might expect that more freedom is needed for a dark energy model to extend this emulation into the nonlinear regime. For example, the  $f(R)$  and DGP models exhibit a chameleonlike behavior [56] in order to restore GR in high-density environments [37,39,42]. To emulate this effect, a dark energy model would also need a chameleonlike coupling to matter [56]. It would be worth studying to what extent general physical constraints can be placed on dark energy models which also apply in the nonlinear regime.

## IV. FORECASTS FOR WEAK LENSING SURVEYS

We now present quantitative forecasts of the constraining power of future surveys with regard to modified gravity. Following the treatment presented in Sec. II, we consider the galaxy-shear and shear-shear correlations,

$C^{g\kappa}$ , and  $C^{\kappa\kappa}$ , on linear scales ( $\ell \lesssim 200$  for  $z \gtrsim 1$ ). In this regime, the Gaussian error estimate is a good approximation. The variance of the cross-correlation  $C^{AB}(\ell)$ , where  $A, B$  stand for any of  $g_i, \kappa_j$ , is then given by:

$$\begin{aligned} [\Delta C^{AB}(\ell)]^2 = & \frac{1}{f_{\text{sky}}(2\ell + 1)} \left\{ \left[ C^{AA}(\ell) + \frac{\sigma_A^2}{n_A} \right] \right. \\ & \left. \times \left[ C^{BB}(\ell) + \frac{\sigma_B^2}{n_B} \right] + C^{AB}(\ell)^2 \right\}. \quad (24) \end{aligned}$$

Here,  $f_{\text{sky}}$  is the fraction of sky observed in the survey,  $n_{A,B}$  denote the number densities of galaxies per sr in each sample, and  $\sigma_{A,B}$  is the shot noise error. For galaxy number counts,  $\sigma_g = 1$ , while for the shear (convergence), we take  $\sigma_\epsilon = 0.35$  as the shot noise due to intrinsic ellipticities. We use the exact integrals [Eqs. (7)–(9)] for the correlations for  $\ell \leq 10$ . For higher  $\ell$ , we use the Limber-approximation expressions [Eqs. (11)–(13)], since the deviations are less than 1% and drop quickly for higher  $\ell$ . Note that in any case the bulk of the signal-to-noise comes from much higher  $\ell$ .

In principle one should take into account magnification bias as well, which adds additional fluctuations to the observed galaxy overdensity and hence affects  $C^{gs}$  and  $C^{g\kappa}$ . For a galaxy population with bias  $b$ , the observed galaxy overdensity  $\delta_g$  will be given by [57]:

$$\delta_g = b\delta + (5s - 2)\kappa, \quad (25)$$

where  $\delta$  is the matter overdensity,  $\kappa$  is the convergence, and  $s = d \lg N / dm$  is the logarithmic number count slope as a function of magnitude  $m$ . Typical values for galaxy surveys are  $s = 0.2, \dots, 0.6$  [57,58]. The galaxy-shear correlation will thus be modified as:

$$C^{g\kappa}(\ell) \rightarrow C^{g\kappa}(\ell) + (5s - 2)C^{\kappa_f \kappa}(\ell), \quad (26)$$

where  $\kappa_f$  is the convergence calculated for the foreground galaxy redshift bin. Note that modified gravity will also affect the magnification bias term. Since we do not have a realistic estimate for the number count slope in the surveys considered here, we do not include this effect. For the galaxy-shear correlation with foreground galaxies centered around  $z = 1.1$  and for the range in  $s$  given above, we estimate that the effect is around 10% ( $\ell \gtrsim 50$ ) for  $\Lambda$ CDM and reaches up to 30% for the  $f(R)$  cosmology. Note that the parameter  $s$  is measurable in surveys. Furthermore, by varying the magnitude cut of the galaxy sample, one can vary  $s$  to some extent and in this way probe the magnification effect. Hence, while straightforward to include for an actual survey, magnification bias will not affect the forecasts presented here appreciably.

Our fiducial flat  $\Lambda$ CDM cosmology is given by:  $\sigma_8 = 0.8$ ,  $\Omega_m = 0.27$ ,  $\Omega_\Lambda = 0.73$ ,  $\Omega_b = 0.046$ ,  $h = 0.7$ ,  $n_s = 0.95$ . For the linear matter power spectrum, we use the transfer function from [59]. The parameters used for the modified gravity models are stated in Sec. III. Additionally,

we will consider a  $\Lambda$ CDM cosmology with a nonlinear power spectrum from HALOFIT [60], in order to assess where the linear approximation breaks down. Note that this is only indicative; nonlinearities can in principle become important already at larger scales in modified gravity theories, due to the nonlinear nature of the modified evolution equations for perturbations.

## A. Survey specifications

We adopt simple survey specifications, as we are mainly interested in the differences between modified gravity models from GR in this paper, which do not depend appreciably on the detailed specifics of the survey. The galaxy redshift distribution  $dN/dz$  is adopted from observations [61,62] for a magnitude-limited sample with  $I < 27$ , as parametrized as ‘‘Sample I’’ in [63]. This is roughly what is expected to be attained by LSST [64] or SNAP [65]. The median redshift of the distribution is 0.91. We then divide the galaxy distribution into redshift bins defined by  $z_l, z_h$ :

$$W_g(z) = C \frac{dN}{dz} \left[ \text{erfc} \left( \frac{z_l - z}{\sqrt{2}\sigma_z} \right) - \text{erfc} \left( \frac{z_h - z}{\sqrt{2}\sigma_z} \right) \right], \quad (27)$$

where  $C$  is a normalization constant,  $\text{erfc}$  is the complementary error function,  $z_l$  and  $z_h$  are the lower and upper bin boundaries, respectively, and  $\sigma_z$  is the expected photometric redshift error. We adopt  $\sigma_z = 0.03(1 + z)$ .

In the following, for studies of the *redshift evolution* of the galaxy-shear and shear-shear correlations, we divide the redshift range from  $z = 0$ –3 in bins with  $\Delta z = z_h - z_l = 0.4$ , so that the first bin is defined by  $z_l = 0$ ;  $z_h = 0.4$ , while the last bin corresponds to  $z_l = 2.4$ ;  $z_h = 2.8$ . In addition, we define a ‘‘background’’ high- $z$  bin encompassing the galaxies from  $z = 3$  to  $z = 5$  (bin ‘‘B’’, with a median redshift  $\bar{z}_b = 3.6$ ). We then correlate foreground galaxies or shear with the shear of galaxies in bin B. For studies of the *scale-dependence* of  $C^{g\kappa}(\ell)$  and  $C^{\kappa\kappa}(\ell)$ , we choose the same background galaxies, and use a wider foreground redshift bin defined by  $z_l = 0.8$ ,  $z_h = 1.6$  (yielding a median redshift of  $z_f = 1.1$ ). The constraints on modified gravity do not depend strongly on the number and precise redshift of the foreground and background bins chosen.

We do not attempt to model the galaxy bias in each bin, instead we show correlations divided by  $b$ , where applicable. In practice, the bias can be taken as free (scale-independent) parameter to be marginalized over. We will see that the dependence on scale and redshift of the effects of modified gravity should allow them to be disentangled from galaxy bias. We will show forecasts for LSST, adopting  $n_g = 50 \text{ arcmin}^{-2}$  as the total observed galaxy density, and  $f_{\text{sky}} = 0.5$  as the observed sky fraction. Constraints similar to those for LSST are expected from the ‘‘wide survey’’ of SNAP [65]. Galaxy-shear and shear-shear correlations offer a large amount of information. As we are



mainly interested in the specific behavior of weak lensing correlations in the different modified gravity models, we do not attempt to fully exploit this information here; instead, we will separately discuss the scale ( $\ell$ ) dependence and redshift evolution of the observables, pointing out generic features of the different model predictions, and whether these effects will be observable in future surveys.

### B. Scale dependence

We first consider the galaxy-shear cross-correlation, correlating foreground galaxies from bin ‘‘F’’ ( $\bar{z}_f = 1.1$ ) with the shear from galaxies in bin B ( $\bar{z}_b = 3.6$ ). Figure 2 (left panel) shows  $C^{g\kappa}(\ell)/b$  for  $\Lambda$ CDM and the modified gravity models, where  $b$  is the bias of the foreground galaxies. There are clear differences in the magnitude of the signal, with the largest correlation coming from the  $f(R)$  model, while DGP and TeVeS yield weaker correlations than the corresponding GR + DE models with identical  $H(z)$  (thin lines). Qualitatively, this is what we expected after the discussion of the models in Sec. III (see also Fig. 1). The differences to the predictions of the GR + DE models with the same expansion history are of order 50% or more in the case of  $f(R)$  and TeVeS, and of order 10% in the case of DGP (right panel of Fig. 2). A scale-dependence of the ratio is also apparent; in the case of the DGP model, the deviations become slightly smaller towards smaller scales, while the opposite scale dependence is apparent for the  $f(R)$  model. This is due to the different values of the metric ratio in the quasistatic (small-scale) regime for the different models (Sec. III). Note that for DGP and  $f(R)$ , we expect the GR behavior to be restored on sufficiently small (nonlinear) scales. In the case of TeVeS, the differences to GR are also sourced by the modified Poisson equation, and hence remain present

even at small scales. Apparently, for the redshift bins chosen, nonlinear evolution becomes relevant for  $\ell \gtrsim 300$  in the  $\Lambda$ CDM case. Hence, any predictions at larger  $\ell$  should not be taken at face value. We found that the deviations from GR in terms of  $R^{g\kappa}(\ell) = C^{g\kappa}(\ell)/\sqrt{C^{gg}(\ell)}$ , which is independent of the linear galaxy bias, are very similar to those of  $C^{g\kappa}$ .

In Fig. 3 we show the corresponding results for the shear-shear correlation of the high- $z$  B bin. The results are quite similar to those for the galaxy-shear correlation. The shear-shear correlation offers the advantage of being independent of any galaxy bias. However, small-scale modes at low redshifts contribute to the shear-shear correlation, so that the effects of nonlinear evolution become relevant already at  $\ell \sim 200$ . In contrast, the contribution to the galaxy-shear correlation we considered is concentrated around  $\bar{z}_f = 1.1$ , where the nonlinear evolution is somewhat less relevant.

Finally, we determine whether the differences in magnitude and scale-dependence of weak lensing correlations will be observable in future surveys. Figure 4 shows the deviations for  $C^{g\kappa}(\ell)$  and  $C^{\kappa\kappa}(\ell)$  for the same redshift bins as above, binned in  $\ell$  with  $\Delta\ell = 50$ . Also shown are  $1\sigma$  statistical errors expected for an LSST-like survey, using Eq. (24). Apparently, the overall difference in the lensing signal is distinguishable at very high significance, to a comparable degree in both galaxy-shear and shear-shear correlations. As both observables are prone to different experimental systematics, the possibility of measuring both correlations in the same survey will enable powerful cross-checks of any signs of deviations from the GR predictions. Choosing a more conservative background redshift bin from  $z = 2$  to 3, with median redshift  $\bar{z}_b = 2.4$ , degrades the expected signal-to-noise of the deviations in  $C^{g\kappa}$  and  $C^{\kappa\kappa}$  by not more than 20%.

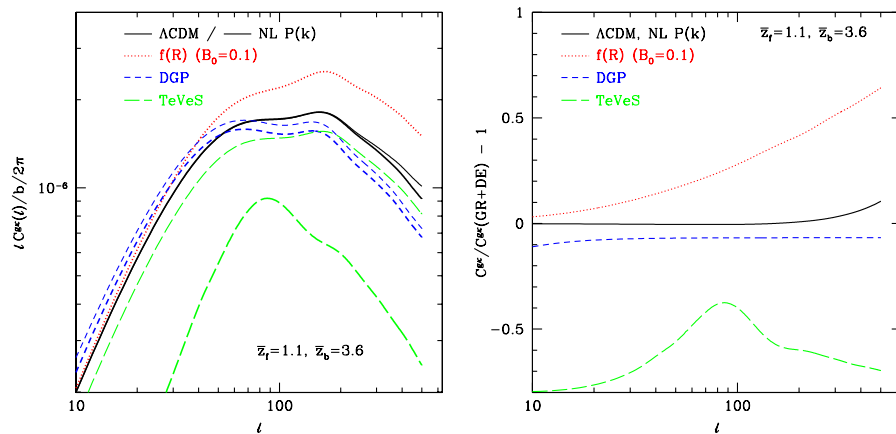


FIG. 2 (color online). Left panel: The galaxy-shear cross power  $C^{g\kappa}(\ell)/b$  for  $\Lambda$ CDM (black/solid line) and modified gravity theories:  $f(R)$  (red/dotted line), DGP (blue/short-dashed line), and TeVeS (green/long-dashed line). In case of DGP and TeVeS, the thin lines show the corresponding predictions for a GR + DE model with the same expansion history. The foreground galaxies are from bin F with median redshift of  $\bar{z}_f = 1.1$ , and background (sheared) galaxies are from bin B with  $\bar{z}_b = 3.6$  (see text). Right panel: Relative deviation of the galaxy-shear cross power  $C^{g\kappa}(\ell)$  of modified gravity models from that of a GR + DE model with identical expansion history, for the same redshift bins as in the left panel.

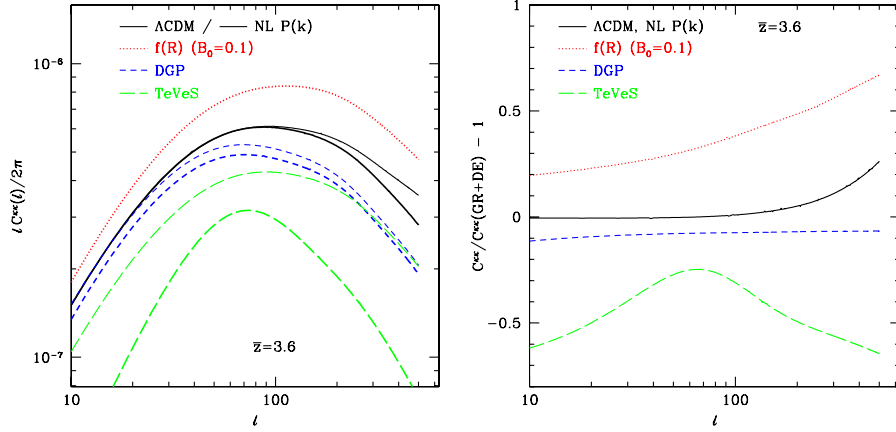


FIG. 3 (color online). Left panel: The shear-shear autocorrelation  $C^{\kappa\kappa}(\ell)$  for  $\Lambda$ CDM and modified gravity theories, for high-redshift galaxies with median redshift  $\bar{z}_b = 3.6$ . The different colors and line styles correspond to the same modified gravity and GR + DE models as in Fig. 2. Right panel: Relative deviation of the shear power spectrum  $C^{\kappa\kappa}(\ell)$  from that of GR + DE models with the same expansion history, for the same high-redshift galaxies as in the left panel.

In addition to the overall magnitude, the different scale dependence of  $C^{g\kappa}(\ell)$  and  $C^{\kappa\kappa}(\ell)$  in the  $f(R)$  and TeVeS models should be clearly distinguishable, while the scale dependence of the deviation of the DGP model might be difficult to detect. A scale dependence of the deviation of lensing correlations from the GR + DE prediction should break degeneracies with other cosmological parameters such as  $b$  and  $\sigma_8$ . The redshift evolution of the lensing signal, to which we now turn, can serve as an additional tool for this purpose.

### C. Redshift evolution

In order to study the redshift evolution of lensing correlations in GR and modified gravity scenarios, we keep the background galaxy bin B ( $z = 3-5$ , median  $\bar{z}_b = 3.6$ ) fixed while considering foreground redshift bins with various median redshifts as explained in Sec. IVA. We keep the width of the foreground redshift bins fixed at  $\Delta z = 0.4$ .

This is only a subset of the cross-correlations possible, which for our purposes serves to show how the evolution of correlations differs in modified gravity theories.

Let us begin with the galaxy-shear correlation, shown in Fig. 5 (left panel) for a fixed  $\ell = 100$  as a function of the median redshift  $\bar{z}_f$  of the foreground galaxies. The overall behavior as a function of  $\bar{z}_f$  is due to the lensing weight function  $W_L$ , which peaks at  $z \sim 0.5$ , corresponding to half of the distance to the lensed galaxies, of order  $\chi(\bar{z}_b)$ . The precise evolution with redshift however depends on the evolution of the potentials  $\propto (1+z)D_m(z)$ , which differs in modified gravity theories (right panel of Fig. 5). We again find the expected result that  $f(R)$  shows a larger lensing signal, while DGP and TeVeS predict smaller lensing signals than the corresponding GR + DE models. In all cases, we see a significant redshift evolution of the deviations. In the case of  $f(R)$  and DGP, the deviations become smaller at higher  $z$ , as GR becomes restored in the

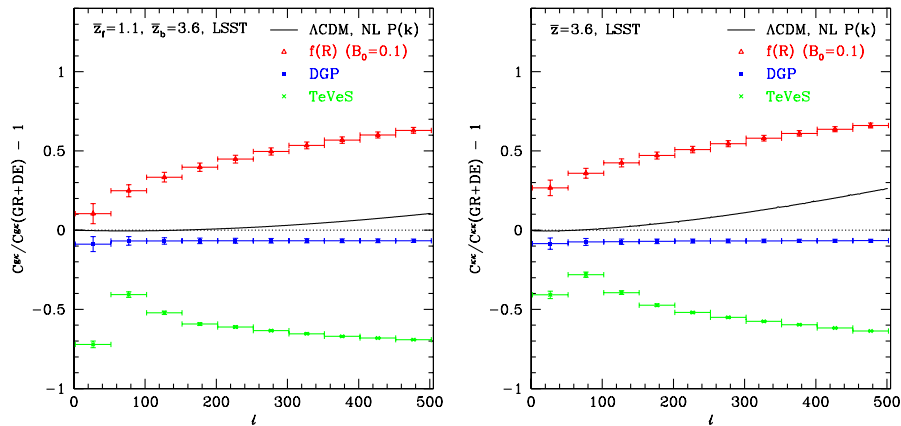


FIG. 4 (color online). Left panel: Relative deviation of the cross power  $C^{g\kappa}(\ell)$  from that of the corresponding GR + DE models, for the same redshift bins as in Fig. 2, but in bins of  $\Delta\ell = 50$  with statistical errors expected from LSST. Right panel: Same as the left panel, but for the shear-shear correlation of high- $z$  galaxies (as in Fig. 3).

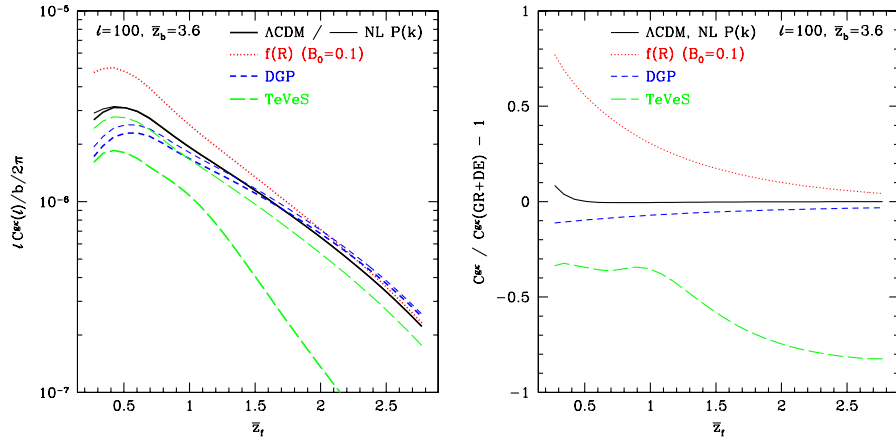


FIG. 5 (color online). Left panel: The galaxy-shear cross power  $C^{g\kappa}(\ell)/b$  at  $\ell = 100$  for a fixed background galaxy sample with median redshift  $\bar{z}_b = 3.6$ , as a function of the redshift  $\bar{z}_f$  of foreground galaxies. The different lines correspond to the same modified gravity and GR + DE models as in Fig. 2. Right panel: Relative deviation of the galaxy-shear power predicted by the modified gravity models from those of the corresponding GR + DE models.

matter-dominated epoch in these models. Thus, ratios of correlations such as  $C^{g\kappa}(\ell; \bar{z}_f = 0.5)/C^{g\kappa}(\ell; \bar{z}_f = 1.5)$  can serve as probes of gravity. A large part of the observational systematics can be expected to drop out in such a ratio, as will the power spectrum normalization  $\sigma_8$ . However, the different galaxy biases of the two foreground samples have to be taken into account. Alternatively, one can measure ratios of  $R^{g\kappa}$  [Eq. (14)] instead of  $C^{g\kappa}$ , where similar deviations from GR are seen. It is apparent that at  $\ell = 100$ , nonlinearities only become important for very low  $z$  foreground galaxies in the galaxy-shear correlation.

The shear-shear correlation shows a complementary redshift evolution, growing with the foreground galaxy redshift  $\bar{z}_f$ , as the amount of mass along the line of sight as well as the geometrical lever arm increase with  $\bar{z}_f$ . The deviations in the predicted redshift evolution of the shear-

shear correlation for modified gravity models are similar in sign and magnitude as those for the galaxy-shear correlation. Again, with its different redshift evolution and set of observational systematics, the shear-shear correlation can serve as a cross-check of the galaxy-shear correlation.

In Fig. 6 we show how precisely the redshift of evolution of  $C^{g\kappa}$  and  $C^{\kappa\kappa}$  is expected to be measurable with a survey like LSST. We assume a bin in  $\ell$  from 50–150, and consider foreground redshift bins spaced by  $\Delta z = 0.4$ , so that these bins are independent. Note however that the background redshift bin is the same in all cases. It is clear that future surveys should be able to resolve the redshift evolution of weak lensing correlations to high precision, and distinguish the models discussed here based on this evolution. This also holds when choosing a lower- $z$  background redshift bin, e.g.  $z = 2$ –3, although the redshift range

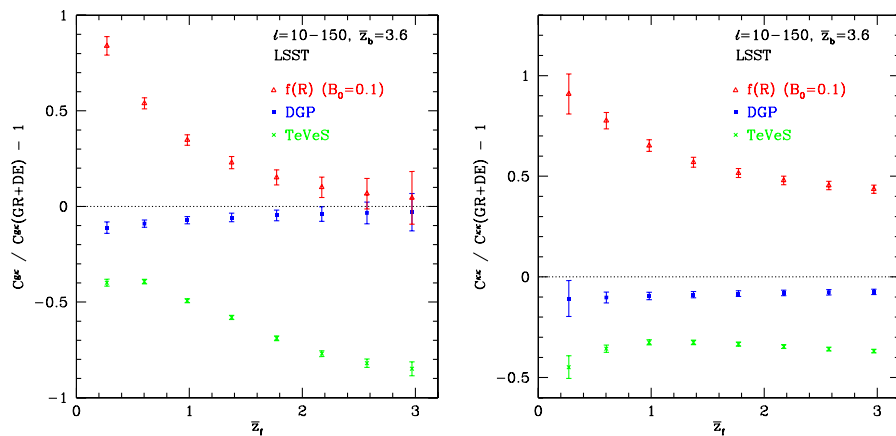


FIG. 6 (color online). Left panel: The relative difference of the galaxy-shear cross power in modified gravity models, as shown in Fig. 5 (right panel), but with statistical error bars expected from LSST. Each point corresponds to an independent foreground galaxy redshift bin with  $\Delta z = 0.4$ ; note that errors are correlated as the same background galaxy sample is used for each point. Right panel: Same as the left panel, but for the shear power spectrum for a fixed high- $z$  redshift bin with  $\bar{z}_b = 3.6$  and the same foreground redshift bins as in the left panel.

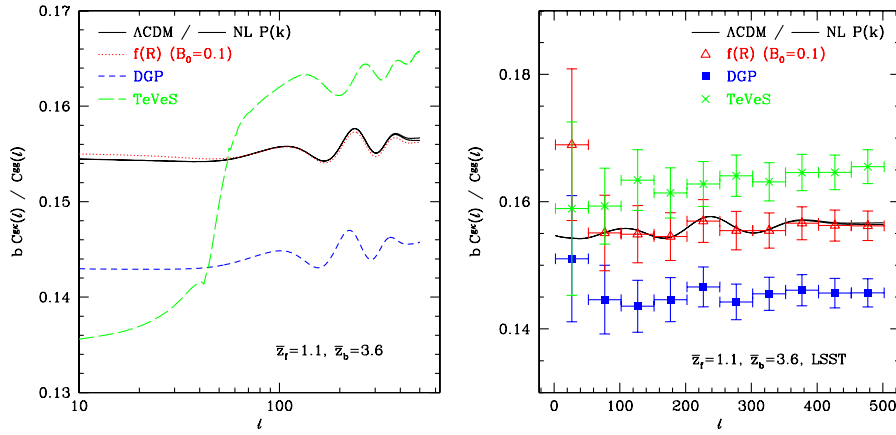


FIG. 7 (color online). Left panel: The “Poisson ratio” of correlations scaled by the bias,  $b\mathcal{P}(\ell)$  [Eq. (17)], for foreground galaxies with mean redshift  $\bar{z}_f = 1.1$  and (sheared) background galaxies with  $\bar{z}_b = 3.6$ , in  $\Lambda$ CDM and modified gravity theories. Right panel: The same as the left panel, in bins of  $\Delta\ell = 50$  and with statistical error bars expected from LSST.

usable for probing the evolution of deviations from GR will be restricted to  $z \lesssim 1.5$  in this case.

#### D. Poisson ratio

We now discuss forecasts for the measurement of the “Poisson ratio”  $\mathcal{P}(\ell) \equiv C^{g\kappa}(\ell)/C^{gg}(\ell)$  presented in section II B. Figure 7 shows  $\mathcal{P}(\ell)$  as a function of  $\ell$  for the foreground galaxy bin F ( $\bar{z}_f = 1.1$ ) and the background bin B ( $\bar{z}_b = 3.6$ ). It is not completely scale-independent even in the case of  $\Lambda$ CDM due to the finite width of the foreground galaxy bin ( $\Delta z = 0.4$ ); in section II B we had assumed a  $\delta$ -distribution in redshift for the foreground galaxies. As expected from Fig. 1, TeVeS shows the largest differences in  $\mathcal{P}(\ell)$ . The modifications to the Poisson equation are very small for the assumed  $f(R)$  model, while the DGP model shows an offset in  $\mathcal{P}(\ell)$  due to the different  $\Omega_m$  adopted for this model (Sec. III B). Some of the generalizations of the DGP model considered in [49] have a modified Poisson equation which should also leave an observable signature in  $\mathcal{P}(\ell)$ .

The right panel of Fig. 7 shows the statistical error expected for LSST on the measurement of  $\mathcal{P}(\ell)$ , in bins of  $\Delta\ell = 50$ . For simplicity, the errors on  $C^{gg}$  and  $C^{g\kappa}$  were assumed to be independent. In this robust test of the Poisson equation, the present TeVeS model should leave an observational signature, as should any modified gravity model that shows modifications to the Poisson equation on the order of 5% or greater. Signatures of appreciable dark energy density perturbations on scales less than  $\sim$ Gpc should be detectable in  $\mathcal{P}(\ell)$  as well.

### V. CONCLUSIONS

Uncovering the physics behind the accelerated expansion of the Universe is one of the most compelling open problems in astrophysics today. One fundamental question to answer is whether the cause lies in an additional component in the energy budget of the Universe, or in a

modification of general relativity on cosmological scales. By considering galaxy-shear and shear-shear correlations on large scales, we showed that weak lensing, with its ability to probe the scale dependence and redshift evolution of the cosmological gravitational potentials and their relation to matter, can serve as a very sensitive probe in discerning between modified gravity and dark energy. We focused on the effects of modified gravity on the growth of structure, effectively assuming that the expansion history is very well constrained through supernovae Ia, the CMB, and baryon acoustic oscillation measurements. In practice, distance and growth measures should be used jointly to place constraints on modified gravity models.

Weak lensing is also a sensitive probe of the background expansion history, both through geometry and the growth of structure. However, when using the growth of structure to infer the background expansion history (parametrized, e.g., by the dark energy equation of state  $w$ ), one relies on the validity of general relativity on cosmological scales: as we have shown here, modified gravity affects the growth of structure and weak lensing observables independently of the expansion history. Fortunately, it is possible to isolate the dependence on the spacetime geometry of lensing observables via shear ratios [40,41]. These techniques will not be affected by modifications to gravity.

By cross-correlating foreground galaxies with the shear of background galaxies, it is possible to probe the relation between matter and potentials, i.e. the Poisson equation. For this purpose, we introduced the weak lensing correlation ratio  $\mathcal{P}(\ell)$  [Eq. (17)], which is, in the limit of narrow redshift bins, independent of growth effects and the matter power spectrum, and thus isolates modifications to the matter-potential relation. However, galaxy-shear correlations necessarily depend on the *a priori* unknown galaxy bias. On linear scales, the degeneracy with the bias can presumably be broken by considering the nontrivial scale dependence of the modified gravity signatures; alternatively, one can consider the reduced correlation,  $R^{g\kappa}(\ell)$

[Eq. (14)]. In contrast, the shear-shear correlation is independent of any galaxy bias, while it is more affected by the nonlinear gravitational evolution at late times. We stress that any modification of gravity should leave a signature in *both* galaxy-shear and shear-shear correlations, and the two methods with their different experimental systematics can serve as cross-checks of the results.

In this paper, we considered three viable modified gravity models which are, in broad terms, consistent with current measurements of the CMB and the expansion history. We compared each model to a GR + DE scenario with identical expansion history, showing that weak lensing can break this degeneracy even in the case of an extremely tightly constrained expansion history. Furthermore, all of these models make definite predictions for weak lensing in the linear regime: the  $f(R)$  model generically predicts a larger lensing signal than expected in GR; the DGP braneworld model predicts a smaller lensing signal than a GR + DE model with the same expansion history; and TeVeS predicts a weaker lensing signal with considerably modified scale dependence. In all cases, these are robust features of the underlying model, linked to the nonzero difference between the cosmological potentials, and modifications to the Poisson equation.

We showed that future wide-field weak lensing surveys, such as LSST and the wide survey of SNAP, can detect deviations in weak lensing correlations predicted by these three models with high significance. As an example, Fig. 8 shows, as a function of  $\ell$ , the signal-to-noise of the deviation of the modified gravity model predictions expected for LSST, in the case of the galaxy-shear correlation. For comparison, we also show the corresponding signal-to-noise expected for the galaxy-CMB cross-correlation induced by the late-time ISW effect, which is clearly much smaller: weak lensing is considerably more powerful in distinguishing modified gravity models from dark energy models with the same expansion history. As these conclusions hold for the three independent modified gravity scenarios considered here, one might expect them to be valid in general for gravity theories that differ significantly from GR on cosmological scales. While constraints similar to those of LSST are expected from other proposed surveys, such as the SNAP wide survey, these conclusions also hold for less demanding survey specifications.

Apart from relying on data from future experiments, progress in the theoretical understanding of modified gravity will be crucial in order to improve on the sensitivity of probes of gravity. Using weak lensing to probe gravity on smaller scales requires that the nonlinear process of structure formation be understood in modified gravity theories. Once this is the case, the amount of useful information for probing gravity grows dramatically, say by raising  $\ell_{\max}$  from a few hundred to greater than 1000. In addition, one

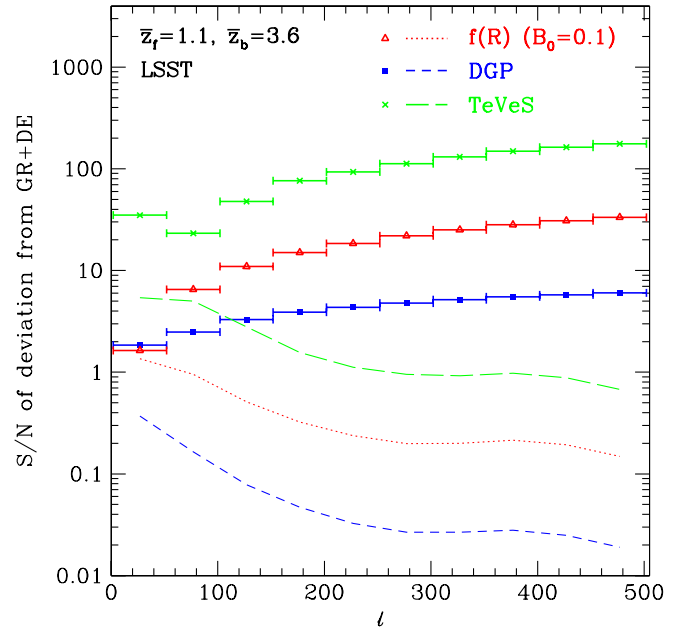


FIG. 8 (color online). Signal-to-noise  $(C^{\text{MG}}(\ell) - C^{\text{GR+DE}}(\ell))/\Delta C^{\text{MG}}(\ell)$  in  $\ell$  bins (points) of the deviation of modified gravity (MG) predictions from GR + DE models with the same expansion history, for the galaxy-shear correlation shown in Fig. 4 (left panel). The lines show the corresponding signal-to-noise of the deviation in the galaxy-CMB cross-correlation via the ISW effect, for the same foreground galaxy redshift bin centered at  $\bar{z}_f = 1.1$ .

might hope that the degeneracy between modified gravity and general, nonsmooth dark energy models present in the linear theory will be broken in the nonlinear regime, at least for a class of dark energy models restricted by physical constraints on, e.g., the coupling to matter.

Finally, we point out that the information in weak lensing correlations should be sufficient to place constraints on “post-GR” parameters independently of an underlying modified gravity theory, especially for the metric ratio  $g(k, z)$  and the rescaled gravitational constant  $G_{\text{eff}}$ . A detailed investigation of this, using all information contained in galaxy and shear correlations, is left for future study.

## ACKNOWLEDGMENTS

I am indebted to Scott Dodelson and Wayne Hu for many valuable suggestions and helpful input. I also thank Michele Liguori for providing the data on the TeVeS model. This work was supported by the Kavli Institute for Cosmological Physics at the University of Chicago through grants NSF PHY-0114422 and NSF PHY-0551142 and an endowment from the Kavli Foundation and its founder Fred Kavli.

- [1] A. G. Riess, L.-G. Strolger, S. Casertano, H. C. Ferguson, B. Mobasher, B. Gold, P. J. Challis, A. V. Filippenko, S. Jha, W. Li, *et al.*, *Astrophys. J.* **659**, 98 (2007).
- [2] M. Kowalski, D. Rubin, G. Aldering, R. J. Agostinho, A. Amadon, R. Amanullah, C. Balland, K. Barbary, G. Blanc, P. J. Challis, *et al.*, arXiv:0804.4142.
- [3] J. Dunkley, E. Komatsu, M. R.olta, D. N. Spergel, D. Larson, G. Hinshaw, L. Page, C. L. Bennett, B. Gold, N. Jarosik, *et al.*, arXiv:0803.0586.
- [4] T. Giannantonio, R. G. Crittenden, R. C. Nichol, R. Scranton, G. T. Richards, A. D. Myers, R. J. Brunner, A. G. Gray, A. J. Connolly, and D. P. Schneider, *Phys. Rev. D* **74**, 063520 (2006).
- [5] D. Pietrobon, A. Balbi, and D. Marinucci, *Phys. Rev. D* **74**, 043524 (2006).
- [6] J. Frieman, M. Turner, and D. Huterer, arXiv:0803.0982.
- [7] B. Jain and P. Zhang, arXiv:0709.2375.
- [8] R. Caldwell, A. Cooray, and A. Melchiorri, *Phys. Rev. D* **76**, 023507 (2007).
- [9] L. Amendola, M. Kunz, and D. Sapone, *J. Cosmol. Astropart. Phys.* **04** (2008) 013.
- [10] E. Bertschinger, *Astrophys. J.* **648**, 797 (2006).
- [11] R. K. Sachs and A. M. Wolfe, *Astrophys. J.* **147**, 73 (1967).
- [12] N. Afshordi, *Phys. Rev. D* **70**, 083536 (2004).
- [13] P. Zhang, *Phys. Rev. D* **73**, 123504 (2006).
- [14] Y.-S. Song, I. Sawicki, and W. Hu, *Phys. Rev. D* **75**, 064003 (2007).
- [15] F. Schmidt, M. Liguori, and S. Dodelson, *Phys. Rev. D* **76**, 083518 (2007).
- [16] P. Zhang, M. Liguori, R. Bean, and S. Dodelson, *Phys. Rev. Lett.* **99**, 141302 (2007).
- [17] Y.-S. Song and K. Koyama, arXiv:0802.3897.
- [18] L. Knox, Y.-S. Song, and J. A. Tyson, *Phys. Rev. D* **74**, 023512 (2006).
- [19] Y.-S. Song, *Phys. Rev. D* **71**, 024026 (2005).
- [20] Y.-S. Song, arXiv:astro-ph/0602598.
- [21] S. Tsujikawa and T. Tatekawa, arXiv:0804.4343.
- [22] W. Hu and I. Sawicki, *Phys. Rev. D* **76**, 104043 (2007).
- [23] E. Bertschinger and P. Zukin, *Phys. Rev. D* **78**, 024015 (2008).
- [24] S. M. Carroll, V. Duvvuri, M. Trodden, and M. S. Turner, *Phys. Rev. D* **70**, 043528 (2004).
- [25] S. M. Carroll, A. De Felice, V. Duvvuri, D. A. Easson, M. Trodden, and M. S. Turner, *Phys. Rev. D* **71**, 063513 (2005).
- [26] Y.-S. Song, W. Hu, and I. Sawicki, *Phys. Rev. D* **75**, 044004 (2007).
- [27] S. Nojiri and S. D. Odintsov, *Int. J. Geom. Methods Mod. Phys.* **4**, 115 (2007).
- [28] M. Amarguioui, Ø. Elgarøy, D. F. Mota, and T. Multamäki, *Astron. Astrophys.* **454**, 707 (2006).
- [29] G. Dvali, G. Gabadadze, and M. Porrati, *Phys. Lett. B* **485**, 208 (2000).
- [30] C. Deffayet, *Phys. Lett. B* **502**, 199 (2001).
- [31] C. Deffayet, G. Dvali, and G. Gabadadze, *Phys. Rev. D* **65**, 044023 (2002).
- [32] J. D. Bekenstein, *Phys. Rev. D* **70**, 083509 (2004).
- [33] S. Dodelson, *Modern Cosmology* (Academic Press., Amsterdam, 2003), p. 440, ISBN .
- [34] M. Bartelmann and P. Schneider, *Phys. Rep.* **340**, 291 (2001).
- [35] W. Hu and B. Jain, *Phys. Rev. D* **70**, 043009 (2004).
- [36] D. Limber, *Astrophys. J.* **119**, 655 (1954).
- [37] I. Navarro and K. Van Acoleyen, *J. Cosmol. Astropart. Phys.* **02** (2007) 022.
- [38] W. Hu and I. Sawicki, *Phys. Rev. D* **76**, 064004 (2007).
- [39] C. Deffayet, G. Dvali, G. Gabadadze, and A. Vainshtein, *Phys. Rev. D* **65**, 044026 (2002).
- [40] B. Jain and A. Taylor, *Phys. Rev. Lett.* **91**, 141302 (2003).
- [41] J. Zhang, L. Hui, and A. Stebbins, *Astrophys. J.* **635**, 806 (2005).
- [42] T. Faulkner, M. Tegmark, E. F. Bunn, and Y. Mao, *Phys. Rev. D* **76**, 063505 (2007).
- [43] R. Bean, D. Bernat, L. Pogosian, A. Silvestri, and M. Trodden, *Phys. Rev. D* **75**, 064020 (2007).
- [44] S. Capozziello and M. Francaviglia, *Gen. Relativ. Gravit.* **40**, 357 (2008).
- [45] G. Cognola, E. Elizalde, S. Nojiri, S. D. Odintsov, L. Sebastiani, and S. Zerbini, *Phys. Rev. D* **77**, 046009 (2008).
- [46] A. Lue, R. Scoccimarro, and G. D. Starkman, *Phys. Rev. D* **69**, 124015 (2004).
- [47] K. Koyama and R. Maartens, *J. Cosmol. Astropart. Phys.* **01** (2006) 016.
- [48] G. Dvali and M. S. Turner, arXiv:astro-ph/0301510.
- [49] K. Koyama, *J. Cosmol. Astropart. Phys.* **03** (2006) 017.
- [50] M. Milgrom, *Astrophys. J.* **270**, 371 (1983).
- [51] C. Skordis, D. F. Mota, P. G. Ferreira, and C. Boehm, *Phys. Rev. Lett.* **96**, 011301 (2006).
- [52] H. Zhao, *Astrophys. J. Lett.* **671**, L1 (2007).
- [53] C. Skordis, *Phys. Rev. D* **74**, 103513 (2006).
- [54] S. Dodelson and M. Liguori, *Phys. Rev. Lett.* **97**, 231301 (2006).
- [55] F. Bourliot, P. G. Ferreira, D. F. Mota, and C. Skordis, *Phys. Rev. D* **75**, 063508 (2007).
- [56] J. Khoury and A. Weltman, *Phys. Rev. D* **69**, 044026 (2004).
- [57] M. LoVerde, L. Hui, and E. Gaztañaga, *Phys. Rev. D* **75**, 043519 (2007).
- [58] L. Hui, E. Gaztañaga, and M. LoVerde, *Phys. Rev. D* **76**, 103502 (2007).
- [59] D. J. Eisenstein and W. Hu, *Astrophys. J.* **496**, 605 (1998).
- [60] R. E. Smith, J. A. Peacock, A. Jenkins, S. D. M. White, C. S. Frenk, F. R. Pearce, P. A. Thomas, G. Efstathiou, and H. M. P. Couchman, *Mon. Not. R. Astron. Soc.* **341**, 1311 (2003).
- [61] A. Gabasch, R. Bender, S. Seitz, U. Hopp, R. P. Saglia, G. Feulner, J. Snigula, N. Drory, I. Appenzeller, J. Heidt, *et al.*, *Astron. Astrophys.* **421**, 41 (2004).
- [62] A. Gabasch, U. Hopp, G. Feulner, R. Bender, S. Seitz, R. P. Saglia, J. Snigula, N. Drory, I. Appenzeller, J. Heidt, *et al.*, *Astron. Astrophys.* **448**, 101 (2006).
- [63] M. LoVerde, L. Hui, and E. Gaztanaga, *Phys. Rev. D* **75**, 043519 (2007).
- [64] <http://www.lsst.org>.
- [65] <http://snap.lbl.org>.